Shape memory polymer-based hybrid honeycomb structures with zero Poisson's ratio and variable stiffness

Jian Huang[a,c], Qiuhua Zhang[a], Fabrizio Scarpa[b,*], Yanju Liu[a], Jinsong Leng[c,*]

[a] *Department of Aerospace Science and Mechanics, No. 92 West Dazhi Street, Harbin Institute of Technology (HIT), P.O. Box 301, Harbin 150080, PR China*

[b] *Advanced Composites Center for Innovation and Science, University of Bristol, Bristol BS8 1TR, UK*

[c] *Center for Composite Materials and Structures, No. 2 Yikuang Street, Science Park of Harbin Institute of Technology (HIT), P.O. Box 301, Harbin, PR China*

Abstract: This work describes the out-of-plane bending performance, shape memory effect and variable stiffness of a zero Poisson's ratio honeycomb structure made from the tessellation of re-entrant hexagons and thin plates. The re-entrant hexagons are fabricated with ABS plastics and the thin plates are made from thermosetting styrene-based shape memory polymers (SMPs). The hexagons and the SMP plates are bonded within the groove joints in the thickness direction of the re-entrant cell units. The re-entrant hexagons generate out-of-plane flatwise compressive stiffness and in-plane compliance, while the SMPs thin plates support out-of-plane flexibility, the shape memory effect and a variable bending stiffness. Because the ABS plastics possesses a significantly higher glass transition temperature than the SMPs, the ZPR honeycomb structure features a higher out-of-plane flexibility when the environmental temperature rises from room temperature to the glass transition temperature of the SMPs. On the contrary, the flatwise compressive stiffness of the ZPR honeycomb remains unchanged. Three-point bending tests have also been performed to determine the out-of-plane bending performance of the ZPR structures at varying temperatures.

Keywords: zero Poisson's ratio; honeycomb; variable stiffness; shape memory polymer; cellular structures.

1. Introduction

Honeycombs have been widely used as core materials in sandwich panels in a wide range of applications, from low-cost doors to advanced aerospace structures. The rationale behind the use of cellular or honeycomb materials is their remarkable lightweight characteristics and tailorable mechanical performances, which are directly dependent upon the topology and size of the unit cell [1]. Flexible honeycomb structures have also been recently proposed as a promising solution for morphing skins, the latter being a critical technology for the design of morphing airframes [2, 3]. Different honeycomb configurations result in different in-plane Poisson's ratios, which lead to multiple deformed shapes when bent out-of-plane [4, 5]. Honeycomb structures with positive Poisson's ratio (PPR) are typical of classical hexagonal honeycombs. The PPR effects manifests in a saddle-shape or anticlastic curvature under out-of-plane deformation, which makes the production of sandwich structures with complex geometry somehow difficult [6, 7]. The re-entrant hexagonal[8, 9],

* Corresponding author

E-mail address: lengjs@hit.edu.cn (Jinsong Leng); f.scarpa@bristol.ac.uk (Fabrizio Scarpa).

hexachiral [10, 11] anti-tetrachiral [12] and tetrachiral [11, 13] honeycombs however exhibit a negative Poisson ratio (NPR) behavior. NPR leads to synclastic curvatures or dome-shaped surfaces when those cellular structures are subjected to an out-of-plane bending deformation. Another subset of cellular structures is the one with zero Poisson's ratio (ZPR). ZPR has been observed in honeycomb configurations like the SILICOMB [14-17], chevron [18-20], and accordion [21]. No lateral coupling behavior can be observed when ZPR honeycombs are loaded uniaxially under in-plane deformations [16]. In the case of out-of-plane loading, honeycombs with ZPR behavior exhibit no synclastic or anticlastic curvatures, rather cylindrical ones [22]. These features (absence of transverse in-plane deformation and cylindrical bending) make ZPR cellular structures an interesting material platform for one-dimensional morphing, the build-up of cylindrical sandwich panels, or morphing structures that undergo cylindrical bending deformations [18, 22]. Honeycomb structures with ZPR property have been also used in biomedical scaffolds [23] and one-dimensional spanwise morphing flexible skins [2, 3, 21]. For all the aforementioned honeycomb structures, the out-of-plane flatwise stiffness inevitably decreases when the out-of-plane flexibility increases when the thickness of the cell wall is minimized. A way to overcome this problem is to develop novel ZPR and NPR honeycomb designs by tessellating thin plates and hexagons and therefore create a unit cell with elements that provide separate functions for the in-plane and out-of-plane load bearing performance [4, 24, 25].

Shape memory polymers (SMPs) are polymeric smart materials with the capacity to recover from temporary shapes to their memorized permanent geometry upon the application of external stimuli [26-32]. The heating activation has frequently been used to trigger the shape memory effect [33-35]. SMPs exhibit brittleness and high Young's modulus below the glass transition temperature, but when heated over a specific temperature tend to be very flexible and produce large strains capability [26]. Due to their variable stiffness and shape memory effect, SMPs have been applied for space deployable structures [36], artificial muscles [37], tissue engineering scaffolds [38] and information carriers [39].

In this work, a honeycomb design with two different materials (ABS plastics and SMPs), zero Poisson's ratio and variable stiffness is proposed. The ZPR effect is created by using a cellular structure made from re-entrant hexagons and thin plates. This honeycomb configuration has two components with different functionalities: the re-entrant hexagons made of ABS plastic provide the in-plane flexibility, while the out-of-plane flatwise compressive stiffness and the SMPs based thin plates generate out-of-plane compliance, a shape memory effect and the bending variable stiffness. Another advantage of this novel hybrid honeycomb design is represented by the out-of-plane flatwise compressive stiffness, which does not change when the bending stiffness varies even by modifying the operational temperature. To demonstrate the mechanical properties of this novel hybrid smart honeycomb, three-point bending tests with an isothermal controlled chamber have been carried out. The tests can demonstrate the out-of-plane bending deformation at different temperatures. Experimental tests to assess the shape memory effect and the variable stiffness

property of the ZPR structures have also been performed.

2. Geometry of the unit cell

Fig. 1 shows the layout of the zero Poisson's ratio honeycomb structure and the geometry of its unit cell. The honeycomb configuration consists of one re-entrant hexagonal unit responsible of the out-of-plane compressive stiffness and the in-plane compliance. Thin plates connect the re-entrant hexagons and provide large out-of-plane flexibility [24]. The two colors in Fig. 1 represent the two different materials used (red for the SMP and blue for the ABS plastics). The thin SMP plates provide the shape memory effect and the variable stiffness of the ZPR honeycomb. The SMP used in this work has a much lower glass transition temperature (T_g) than the ABS plastics, and it is therefore reasonable to infer that the ABS plastic will not be affected when the temperature reaches the T_g of the SMPs. In this way, the variable bending stiffness of the ZPR honeycomb structure can be obtained by the increment of the temperature, while its flatwise compressive stiffness remains the same. The hexagons have inclined walls with equal length l and vertical walls with the same length $h=\alpha l$. The thickness of the wall of the re-entrant hexagons is represented by the parameter βl, while the inclined wall has a tilt angle θ. The parameter γl represents the height of the re-entrant hexagons, which also represents the height of the ZPR honeycomb structures along the 3-direction. The thin plate has a length $(\eta+\beta)l$, a thickness of λl, and a width that equals the length of the vertical wall. The thin plate has also a bonding area that shapes into an anti-parallelogram. The vertical walls of the re-entrant hexagons along the thickness direction feature key grooves to bond the two parts together.

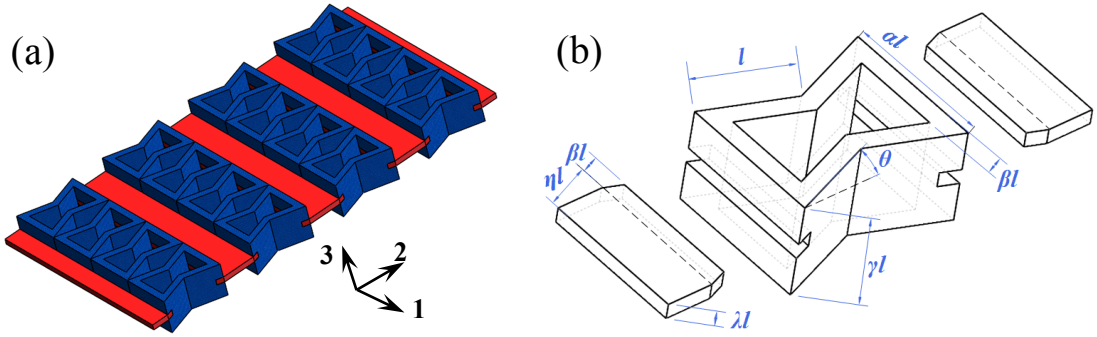

Fig. 1 Layout of the hybrid ZPR SMP/ABS honeycombs and the geometry of its unit cell.

3. Basic mechanical tests of the SMPs

Thermosetting styrene-based SMPs have been used in this work to manufacture the thin plate part of the ZPR honeycomb structures. The detailed synthesis and curing processes have been reported in Ref. [40]. In order to characterize the glass transition temperature of the SMP material, rectangular plate samples with dimensions of 30mm ×5mm×1.6mm have been used to perform a dynamic mechanical analysis (DMA). The tests have been performed using a dynamic mechanical analyzer Q800 from TA Instruments Corp. (USA) in tension mode with a constant heating rate of 5°C/min and

a loading frequency of 1 Hz from 0°C to 100°C. The storage modulus and tanδ of the styrene-based SMPs versus the environmental temperature are shown in Fig. 2. One can readily observe the presence of a glass transition temperature of 55°C. When the temperature increases from 0°C to 97.6°C the storage modulus shows a substantial decrease from to 1460 MPa to 0.8 MPa, meaning that the styrene-based SMP materials is very suitable for the variable stiffness applications.

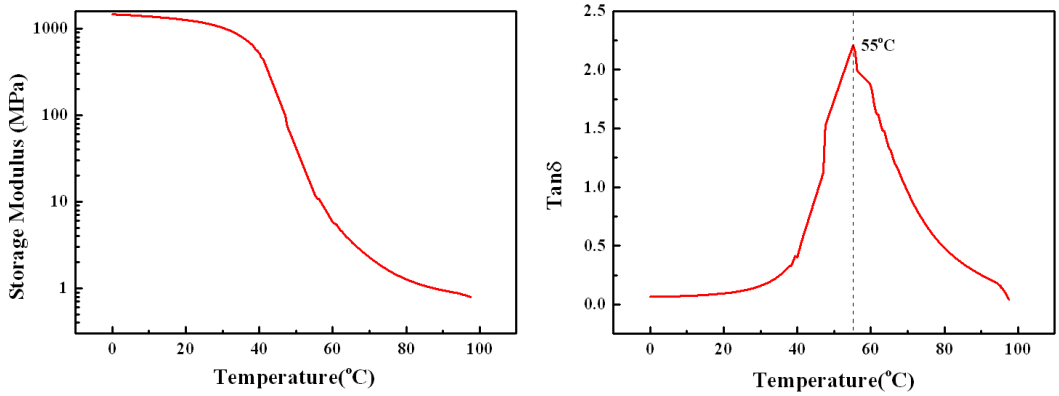

Fig. 2 The storage modulus and tanδ of the styrene-based SMP versus temperature.

4. Manufacturing of the SMPs based ZPR honeycomb structures

The manufacturing of the shape memory polymers based ZPR honeycombs can be divided into four steps: 1) preparation of the re-entrant hexagons; 2) production of a large SMP plate with specific thickness; 3) cutting of the SMP plate into strips with designed geometrical shapes; 4) bonding of the re-entrant hexagons and strips into the specific pattern by using thermal-resistant glue. Vacuum casting technology has been adopted in the preparation of the re-entrant hexagons (Fig.3). Master models have been made with photosensitive resin using a 3D printing machine RSPro450 (UnionTech Corp., Shanghai). The master models have then been placed into a mold casting frame, which was then filled with silicone rubber mixtures. Once cured and dry, the silicone rubber mold was then removed from the casting frame and was also cut into two parts along the parting line. As a following step the master models were removed and the silicone rubber mold was ready for the production of the re-entrant hexagons. The resin of the ABS plastic was then poured into the prepared mold under vacuum conditions. Once casted, the mold has been placed into a heating chamber for curing. The cured re-entrant hexagon was then removed and the silicone rubber mold was ready to reproduce another replica. To ensure the presence of smooth surfaces, all the prepared re-entrant hexagons have been post-processed with sand paper. This vacuum casting procedure has been done using a 3D printing platform (www.mohou.com). The nominal mechanical properties of the ABS plastics used are a Young's modulus E=2000MPa, Poisson's ratio 0.39, tensile strength 30Mpa, density 1020Kg/m^3 and a glass transition temperature of 109°C. After being produced, the SMP plate has been cut into designed strips using a laser cutter. The final step of the production of the honeycombs consisted in bonding the re-entrant hexagons and the thin strips into the tessellation forming the ZPR honeycomb configuration. During this

assembly phase the bonding was provide by a cyanoacrylate adhesive (Yuwang Group, China) with fast curing at room temperature. Medical syringes have been used to distribute the adhesive in an accurate and efficient way.

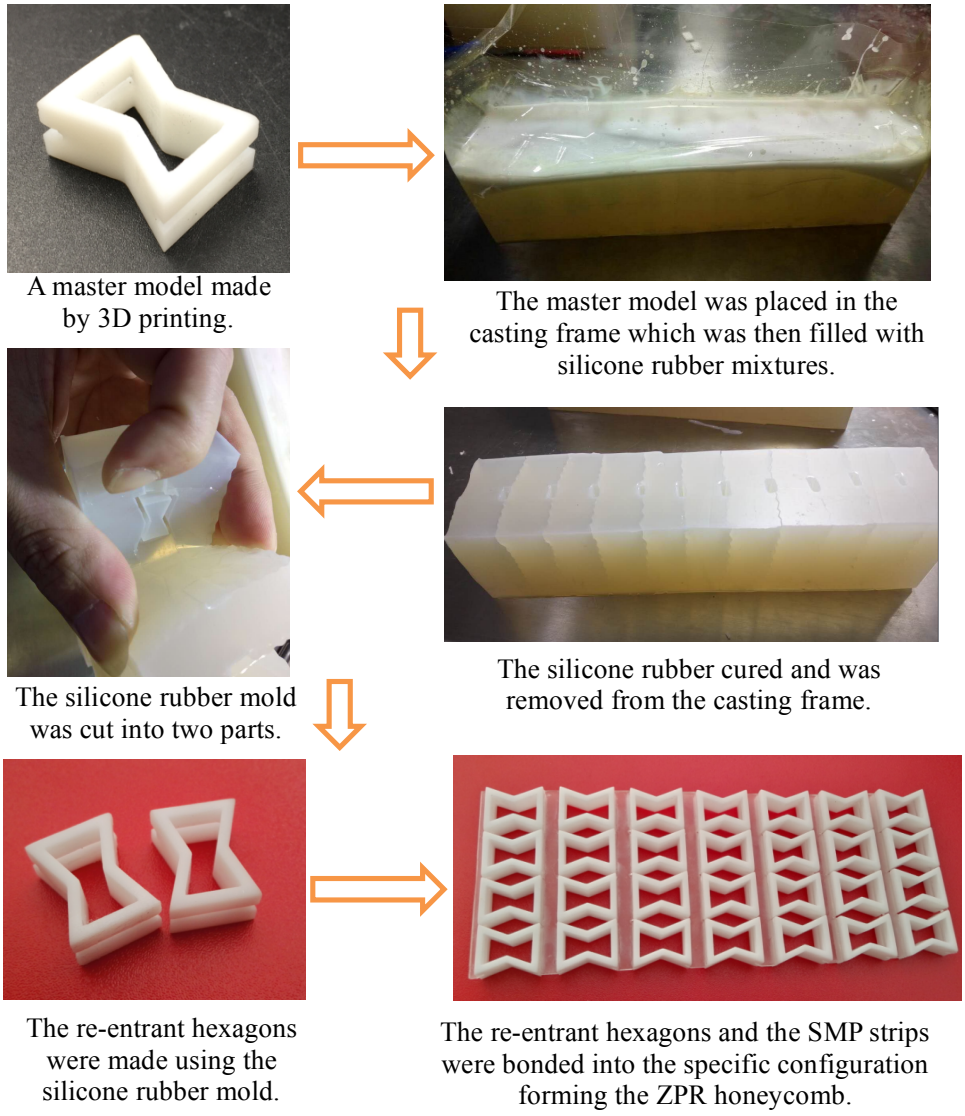

Fig. 3 The manufacturing of the hybrid ZPR honeycomb structures.

5. Three point bending tests

In order to determine the bending performance of the proposed ZPR honeycomb structures, three-point bending tests have been designed and carried out to estimate the variation of the bending modulus versus the temperature. The experimental setup is shown in Fig. 4(a). A thermal controlled chamber allows achieving isothermal conditions at different temperatures. Samples with dimensions of 166mm×60mm×10mm have been used in the tests. Each specimen consisted in four complete unit cells along the width and seven along the span direction. The unit cells had dimensions of l=10mm, and were defined by the nondimensional parameters α=1.5, β=0.2, γ=1.0, η=0.25, λ= 0.16, θ=20° (see Fig. 1(b)). The bending tests were performed using a Zwick/Roell Z010 testing machine with a 1KN load cell. A

displacement rate of 10mm/s and a span length of 143mm have been adopted. The tests have been stopped at a maximum central point deflection of 30mm. Temperatures from 15°C to 35°C with an increment of 5°C have been controlled in the tests. The curves of the loading force versus the central point deflection at different temperatures are shown in Fig. 4(b). The 3P bending trials stopped at 35°C because higher temperatures could produce a faster creep deformation than the applied displacement rate. As an evidence of this phenomenon, a very large creep deformation has been observed after 60 seconds at 40°C (Fig. 5). The equivalent bending modulus E_b of the hybrid SMPs based ZPR honeycomb structures has been calculated with the standard engineering beam expression [41]:

$$d = \frac{Wl^3}{48E_bI} \tag{1}$$

Where d is the deflection at the center of the span width, W and l the loading force and the length of the span. The W/d relation has been extrapolated from the initial linear slope of the curves for each of the five specimen produced. The results of the equivalent bending modulus form the 3P bending tests are shown in Fig. 4(c). A decrement from 10.4 MPa to 0.3 MPa has been observed when the temperature of the isothermal controlled chamber increased from 15°C to 35°C. A temperature change of 20°C results therefore results in a variable stiffness increment of more than 30 times.

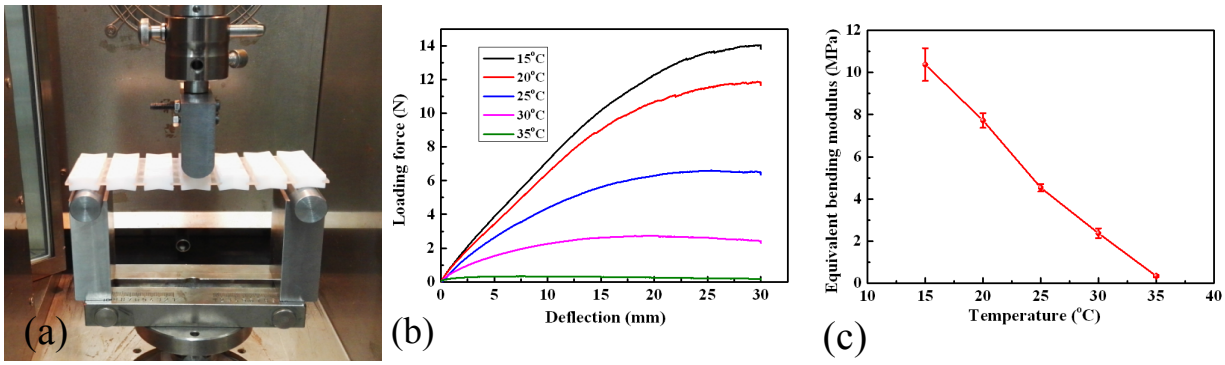

Fig. 4 (a) The experimental setup of the three-point bending tests; (b) the force-deflection curve generated from the tests; (c) the equivalent bending modulus of the ZPR structures vs the isothermal temperature.

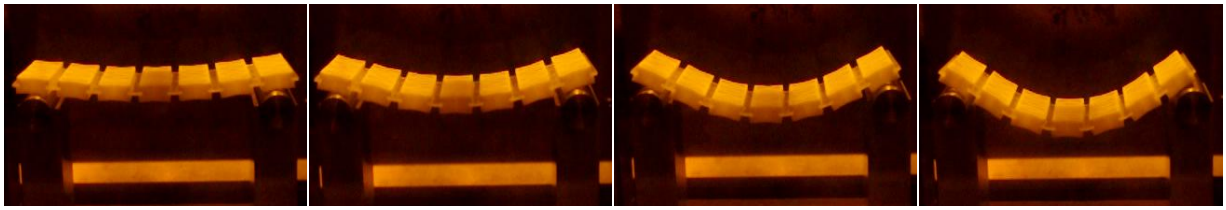

Fig. 5 The creep deformation of the ZPR honeycomb structures under 40°C isothermal environments.

6. Experimental tests of the shape memory effect

SMPs are polymeric smart materials that possess remarkable recovery ability. They also exhibit a good shape memory effect, which makes them able to return from a temporary or deformed, to permanent or original shape by an external (mainly thermal) stimulus. The styrene-based SMPs have a glass transition temperature of 55°C while the ABS plastics one is at 109°C. This feature makes the SMPs turn from hard to soft and start the shape recovery procedure leaving the ABS plastics unaffected when the environmental temperature rises to ~55°C. An experimental test has been performed to determine the shape memory effect of these hybrid ZPR honeycombs. Samples with 4×7 unit cells have been produced with a specific original shape (l=10mm, α=1.5, β=0.2, γ=1.0, η=0.5, λ= 0.16, θ=20°). During the tests the thermal stimulus was constituted by a heating gun, while the surrounding air of the test room provided the cooling. A typical shape recovery process has been observed and shown in Fig. 6. The process can be divided into two heating and one cooling down steps. During the first step the application of the heating is made on the original shape until the SMP thin plates turn soft. The honeycomb is then loaded with a constant external force to achieve a temporary Ω-shape with a very large out-of-plane bending deformation, while decreasing the temperature to room conditions by natural convection. A new deformed temporary shape has been therefore obtained. The next consists in heating again the system with the heating gun and return the honeycomb to the original shape. The whole recovery process from the temporary Ω-shape to the original honeycomb plate system takes about 46s with a 100% recovery.

7. Experimental tests of the variable stiffness property

Although the three-point bending tests have shown the variable stiffness property of the hybrid SMPs based ZPR honeycomb structures, they cannot be efficiently used to predict the mechanical performance of the ZPR honeycombs in practical applications where no ideal isothermal environment exists. To this end we have performed experimental tests related to simply supported honeycomb beams to demonstrate the variable stiffness property at room temperature. Polyimide (PI) heating films with appropriate geometrical dimensions have been chosen as heating method. The maximum applied voltage to the PI films is 12V with a corresponding maximum heating power of 18W. As shown in Fig. 7(a), the PI heating films have been bonded on the bottom surface of the SMP thin plates using 3M adhesive. At room temperature a weight of 500g has been loaded on the center span (170mm – Fig. 7(b)). An average deflection of 5.5mm has been measured; by using Equation (1) the equivalent bending modulus Eb of the hybrid ZPR structure has been estimated at 18.6 MPa.

According to the three-point bending and static tensile tests from Ref. [42], the bending stiffness of the ZPR structures can be very small when the temperature reaches the glass transition temperature of the SMPs. Therefore, no weights have been applied during the heating process and its self-weight has been judged adequate to produce large bending deformations. In order to measure the heating efficiency of the PI heating films, an infrared temperature camera (VarioCAM HiRes sl, JENOPTIK

Infra Tec) has been employed in the tests with a frame rate of 1 Hz. At the meantime, a Canon camera has been placed directly on the front of the honeycomb beam to record the whole deformation process. Voltages of 6V, 9V, 12V have been applied during the heating process using a stabilized voltage supply (ITECH DC Source Meter, IT6154). Fig. 8 shows the whole heating process of the PI films and the bending deformation of the ZPR structures with different applied voltages. For a 9V voltage it has been possible to observe a larger bending deformation than in the 6V case, with almost uniform temperature distributions on the SMP thin plates (Fogs. 8(a) and 8(b)). When 12V were applied, a significantly higher temperature has been measured after 20s, however the bending deformation remained almost the same as the 9V case between 15s and 20s (Fig. 8(c)). This fact can be explained by observing the results from the DMA tests and the static tensile modulus as determined in Ref.[42]. When the temperature reaches the SMP T_g the Young's modulus is quite very small and stays almost the same even when the temperature increases. At room temperature the honeycomb beam is able to withstand a 500g weight loading at the center of the span. When heating up is produced its self-weight (56.8g, including the PI films and wires) can produce very large bending deformations. The large variable stiffness of this honeycomb design can be potentially repeated in real applications with different heating and cooling methods.

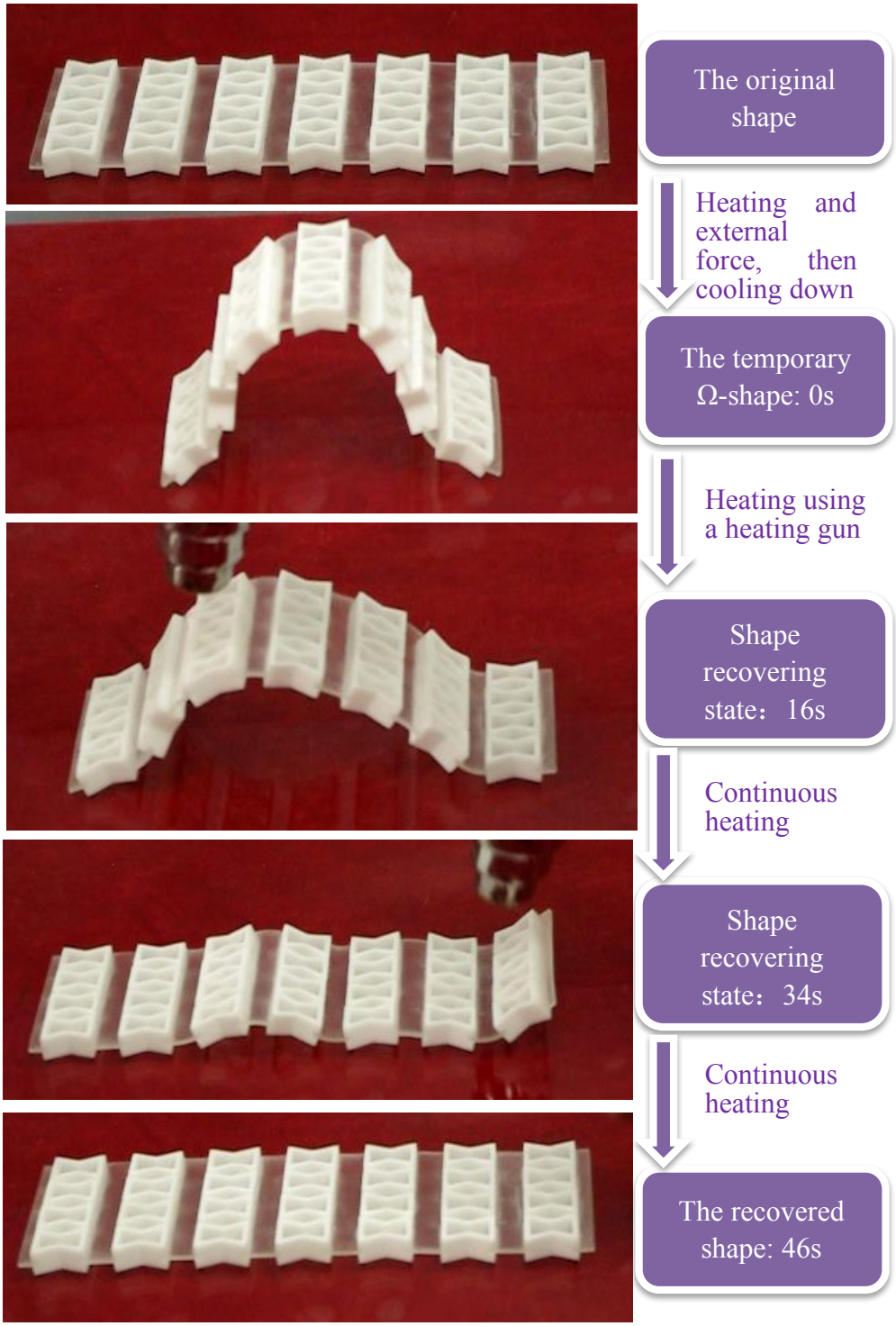

Fig. 6 A typical shape recovery process of the SMPs based ZPR honeycomb structures

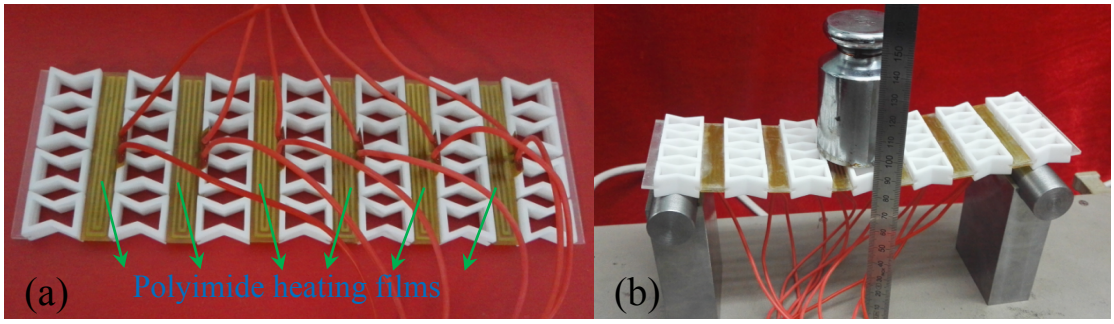

Fig. 7 The sample bonded with PI heating films and the simply supported honeycomb beam.

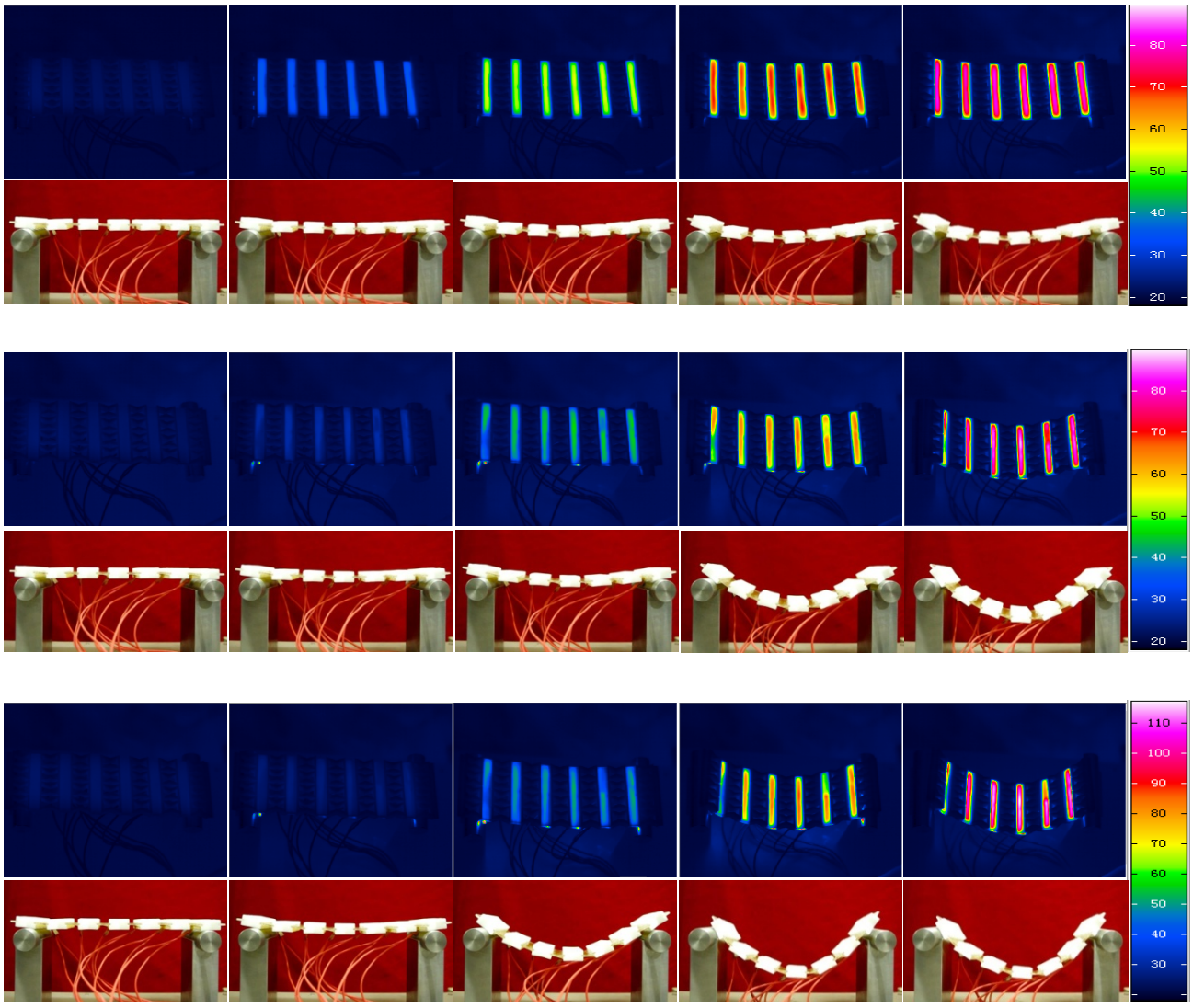

Fig. 8 The heating performance of the PI films and the bending deformation of the hybrid ZPR structures for different applied voltages: (a) 6V; (b) 9V; (c) 12V;

8. Conclusions

We have proposed hybrid ZPR honeycomb structures using the configuration of tessellation of the re-entrant hexagons and thin plates fabricated with two different materials. The ABS plastics re-entrant hexagons were produced using a vacuum casting technology, and thermoset styrene-based SMPs were used for the thin plates. The hybrid ZPR honeycombs are stiff at low temperature and become compliant when the temperature rises. A variable bending stiffness of the ZPR structures has been produced by applying increments of the environmental temperature, leaving the flatwise compressive stiffness of the honeycomb unaffected. Experimental tests have shown that heating and cooling, with different methods that could be evaluated for real applications, can achieve a variable stiffness. The shape memory effect tests show that the hybrid ZPR honeycomb structures recovers from the a temporary Ω-shape to its original shape in 46 seconds with a 100% recovery rate.

Acknowledgements

The support of the FP7-AAT.2012.6.3-1-341509 MORPHELLE and the National Natural Science Foundation of China (Grant No.11225211) are gratefully acknowledged. Jian Huang would also like to thank Mr. Wenbing Li, Mr. Qiwei Zhang and Mr. Jinrong Li for their help with the SMP materials and the experimental tests. Thanks also go to Mr. Yanan Li (www.mohou.com) for his help with the vacuum casting technology.

References:

[1] Gibson LJ, Ashby MF. Cellular solids: structure and properties: Cambridge university press, 1997.

[2] Bubert EA, Woods BK, Lee K, Kothera CS, Wereley NM. Design and fabrication of a passive 1D morphing aircraft skin. Journal of Intelligent Material Systems and Structures. 2010;21:1699-717.

[3] Olympio KR, Gandhi F. Flexible Skins for Morphing Aircraft Using Cellular Honeycomb Cores. Journal of Intelligent Material Systems and Structures. 2009;21:1719-35.

[4] Huang J, Gong X, Zhang Q, Scarpa F, Liu Y, Leng J. In-plane mechanics of a novel zero Poisson's ratio honeycomb core. Composites Part B: Engineering. 2016;89:67-76.

[5] Gong X, Huang J, Scarpa F, Liu Y, Leng J. Zero Poisson’s ratio cellular structure for two-dimensional morphing applications. Composite Structures. 2015;134:384-92.

[6] Evans K. The design of doubly curved sandwich panels with honeycomb cores. Composite Structures. 1991;17:95-111.

[7] Masters I, Evans K. Models for the elastic deformation of honeycombs. Composite Structures. 1996;35:403-22.

[8] Scarpa F, Tomlin P. On the transverse shear modulus of negative Poisson’s ratio honeycomb structures. Fatigue & Fracture of Engineering Materials & Structures. 2000;23:717-20.

[9] Bezazi A, Scarpa F, Remillat C. A novel centresymmetric honeycomb composite

structure. Composite Structures. 2005;71:356-64.
[10] Prall D, Lakes R. Properties of a chiral honeycomb with a Poisson's ratio of—1. International Journal of Mechanical Sciences. 1997;39:305-14.
[11] Miller W, Smith C, Scarpa F, Evans K. Flatwise buckling optimization of hexachiral and tetrachiral honeycombs. Composites Science and Technology. 2010;70:1049-56.
[12] Chen Y, Scarpa F, Liu Y, Leng J. Elasticity of anti-tetrachiral anisotropic lattices. International Journal of Solids and Structures. 2013;50:996-1004.
[13] Lorato A, Innocenti P, Scarpa F, Alderson A, Alderson K, Zied K, et al. The transverse elastic properties of chiral honeycombs. Composites Science and Technology. 2010;70:1057-63.
[14] Chen Y, Scarpa F, Remillat C, Farrow I, Liu Y, Leng J. Curved Kirigami SILICOMB cellular structures with zero Poisson's ratio for large deformations and morphing. Journal of Intelligent Material Systems and Structures. 2013:1045389X13502852.
[15] Lira C, Scarpa F, Olszewska M, Celuch M. The SILICOMB cellular structure: Mechanical and dielectric properties. physica status solidi (b). 2009;246:2055-62.
[16] Lira C, Scarpa F, Tai Y, Yates J. Transverse shear modulus of SILICOMB cellular structures. Composites Science and Technology. 2011;71:1236-41.
[17] Virk K, Monti A, Trehard T, Marsh M, Hazra K, Boba K, et al. SILICOMB PEEK Kirigami cellular structures: mechanical response and energy dissipation through zero and negative stiffness. Smart Materials and Structures. 2013;22:084014.
[18] Grima JN, Oliveri L, Attard D, Ellul B, Gatt R, Cicala G, et al. Hexagonal Honeycombs with Zero Poisson's Ratios and Enhanced Stiffness. Advanced Engineering Materials. 2010;12:855-62.
[19] Grima JN, Attard D. Molecular networks with a near zero Poisson's ratio. physica status solidi (b). 2011;248:111-6.
[20] Attard D, Grima JN. Modelling of hexagonal honeycombs exhibiting zero Poisson's ratio. physica status solidi (b). 2011;248:52-9.
[21] Olympio KR, Gandhi F. Zero Poisson's Ratio Cellular Honeycombs for Flex Skins Undergoing One-Dimensional Morphing. Journal of Intelligent Material Systems and Structures. 2009;21:1737-53.
[22] Neville R, Monti A, Hazra K, Scarpa F, Remillat C, Farrow I. Transverse stiffness and strength of Kirigami zero-ν PEEK honeycombs. Composite Structures. 2014;114:30-40.
[23] Engelmayr GC, Jr., Cheng M, Bettinger CJ, Borenstein JT, Langer R, Freed LE. Accordion-like honeycombs for tissue engineering of cardiac anisotropy. Nat Mater. 2008;7:1003-10.
[24] Huang J, Zhang Q, Scarpa F, Liu Y, Leng J. Bending and benchmark of zero Poisson's ratio cellular structures. Composite Structures. 2016;152:729-36.
[25] Huang J, Zhang Q, Scarpa F, Liu Y, Leng J. In-plane elasticity of a novel auxetic honeycomb design. Composites Part B: Engineering. 2017;110:72-82.
[26] Leng J, Lan X, Liu Y, Du S. Shape-memory polymers and their composites: Stimulus methods and applications. Progress in Materials Science. 2011;56:1077-135.

[27] Li W, Liu Y, Leng J. Selectively actuated multi-shape memory effect of a polymer multicomposite. Journal of Materials Chemistry A. 2015;3:24532-9.
[28] Wang W, Liu Y, Leng J. Recent developments in shape memory polymer nanocomposites: Actuation methods and mechanisms. Coordination Chemistry Reviews. 2016;320–321:38-52.
[29] Huang W, Yang B, An L, Li C, Chan Y. Water-driven programmable polyurethane shape memory polymer: demonstration and mechanism. Applied Physics Letters. 2005;86:114105.
[30] Gall K, Dunn ML, Liu Y, Finch D, Lake M, Munshi NA. Shape memory polymer nanocomposites. Acta materialia. 2002;50:5115-26.
[31] Yao Y, Zhou T, Wang J, Li Z, Lu H, Liu Y, et al. 'Two way' shape memory composites based on electroactive polymer and thermoplastic membrane. Composites Part A: Applied Science and Manufacturing. 2016;90:502-9.
[32] Chen L, Li W, Liu Y, Leng J. Nanocomposites of epoxy-based shape memory polymer and thermally reduced graphite oxide: Mechanical, thermal and shape memory characterizations. Composites Part B: Engineering. 2016;91:75-82.
[33] Behl M, Lendlein A. Shape-memory polymers. Materials today. 2007;10:20-8.
[34] Xie T. Tunable polymer multi-shape memory effect. Nature. 2010;464:267-70.
[35] Xu J, Song J. High performance shape memory polymer networks based on rigid nanoparticle cores. Proceedings of the National Academy of Sciences. 2010;107:7652-7.
[36] Lan X, Liu Y, Lv H, Wang X, Leng J, Du S. Fiber reinforced shape-memory polymer composite and its application in a deployable hinge. Smart Materials & Structures. 2009;18.
[37] Chung T, Rorno-Uribe A, Mather PT. Two-way reversible shape memory in a semicrystalline network. Macromolecules. 2008;41:184-92.
[38] Neuss S, Blomenkamp I, Stainforth R, Boltersdorf D, Jansen M, Butz N, et al. The use of a shape-memory poly (ε-caprolactone) dimethacrylate network as a tissue engineering scaffold. Biomaterials. 2009;30:1697-705.
[39] Sun L, Huang W, Lu H, Wang C, Zhang J. Shape memory technology for active assembly/disassembly: fundamentals, techniques and example applications. Assembly Automation. 2014;34:78-93.
[40] Zhang D, Liu Y, Yu K, Leng J. Influence of cross-linking agent on thermomechanical properties and shape memory effect of styrene shape memory polymer. Journal of Intelligent Material Systems and Structures. 2011:1045389X11425282.
[41] Young WC, Budynas RG. Roark's formulas for stress and strain: McGraw-Hill New York, 2002.
[42] Du H, Liu L, Zhang F, Zhao W, Leng J, Liu Y. Thermal-mechanical behavior of styrene-based shape memory polymer tubes. Polymer Testing. 2017;57:119-25.